UCRL- 85827
PREPRINT
CONF-810511--3

FORMATION AND CONTROL OF PLASMA POTENTIALS IN TMX UPGRADE

T. C. Simonen, T. J. Orzechowski,
M. Porkolab, and B. W. Stallard

This paper was prepared for submittal to
Workshop on Ambipolar Potential Formation
and Control in Bumpy Tori and Mirrors,
Oak Ridge National Laboratory,
Oak Ridge, Tennessee, May 11-12, 1981

May 6, 1981

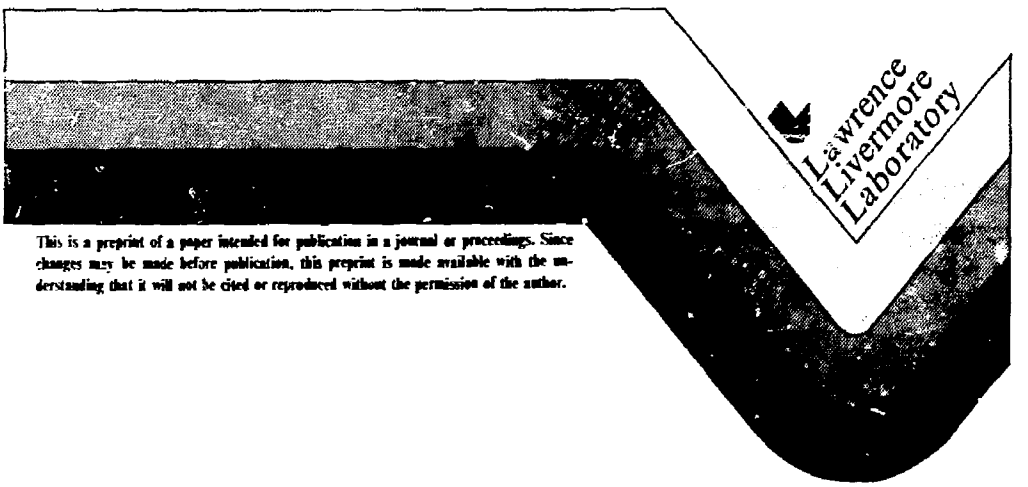

FORMATION AND CONTROL OF PLASMA POTENTIALS IN TMX UPGRADE*

T. C. Simonen, T.J. Orzechowski, M. Porkolab†, and B. W. Stallard
Lawrence Livermore National Laboratory, University of California,
Livermore, California 94550

ABSTRACT

The methods to be employed to form and control plasma potentials in the TMX Upgrade tandem mirror with thermal barriers are described. ECRH-generated mirror-confined electron plasmas are used to establish a negative potential region to isolate the end-plug and central-cell electrons. This thermal isolation will allow a higher end-plug electron temperature and an increased central-cell confining potential. Improved axial central-cell ion confinement results since higher temperature central-cell ions can be confined.

This paper describes: (1) calculations of the sensitivity of barrier formation to vacuum conditions and to the presence of impurities in the neutral beams, (2) calculations of microwave penetration and absorption used to design the ECRH system, and (3) techniques to limit electron runaway to high energies by localized microwave beams and by relativistic detuning.

I. PHYSICS OBJECTIVES OF TMX UPGRADE

The TMX experiment successfully demonstrated that the tandem-mirror configuration could be generated and sustained by neutral-beam injection and that confinement of both ions and electrons was improved over that in single mirrors. The TMX Upgrade will verify that the addition of thermal barriers to the tandem mirror will improve potential confinement and thus increase the attractiveness of the tandem-mirror reactor concept. TMX Upgrade is the first complete tandem-mirror thermal-barrier system. An added and necessary feature of TMX Upgrade is that it is designed to avoid microinstabilities.

The advantage of the thermal-barrier tandem over a basic tandem such as TMX is illustrated by the relative magnitudes of the confining potential wells, which are shown to scale in Fig. 1. This figure shows that a depression in plasma potential ϕ_b isolates the plug electrons, with density and temperature n_p and T_{ep}, from the central-cell electrons, with density and temperature n_c and T_{ec}. If the density of electrons passing between these two regions, n_b^*, is sufficiently small, a large electrostatic potential barrier ϕ_c can be generated by using ECRH to raise T_{ep}. As ϕ_c is increased, higher energy central-cell ions are electrostatically confined. Central-cell confinement improves with higher central-cell temperatures. An unequivocal demonstration of the thermal-barrier concept will be an improvement in plasma confinement in TMX Upgrade relative to TMX.

The two physics objectives of TMX Upgrade are:

1. Investigate a complete tandem-mirror thermal-barrier system.
   - Achieve microstability.
   - Maintain MHD stability.
   - Generate potential profiles by electron heating.
   - Control axial electron temperature gradients.
2. Improve tandem mirror performance over that of TMX.

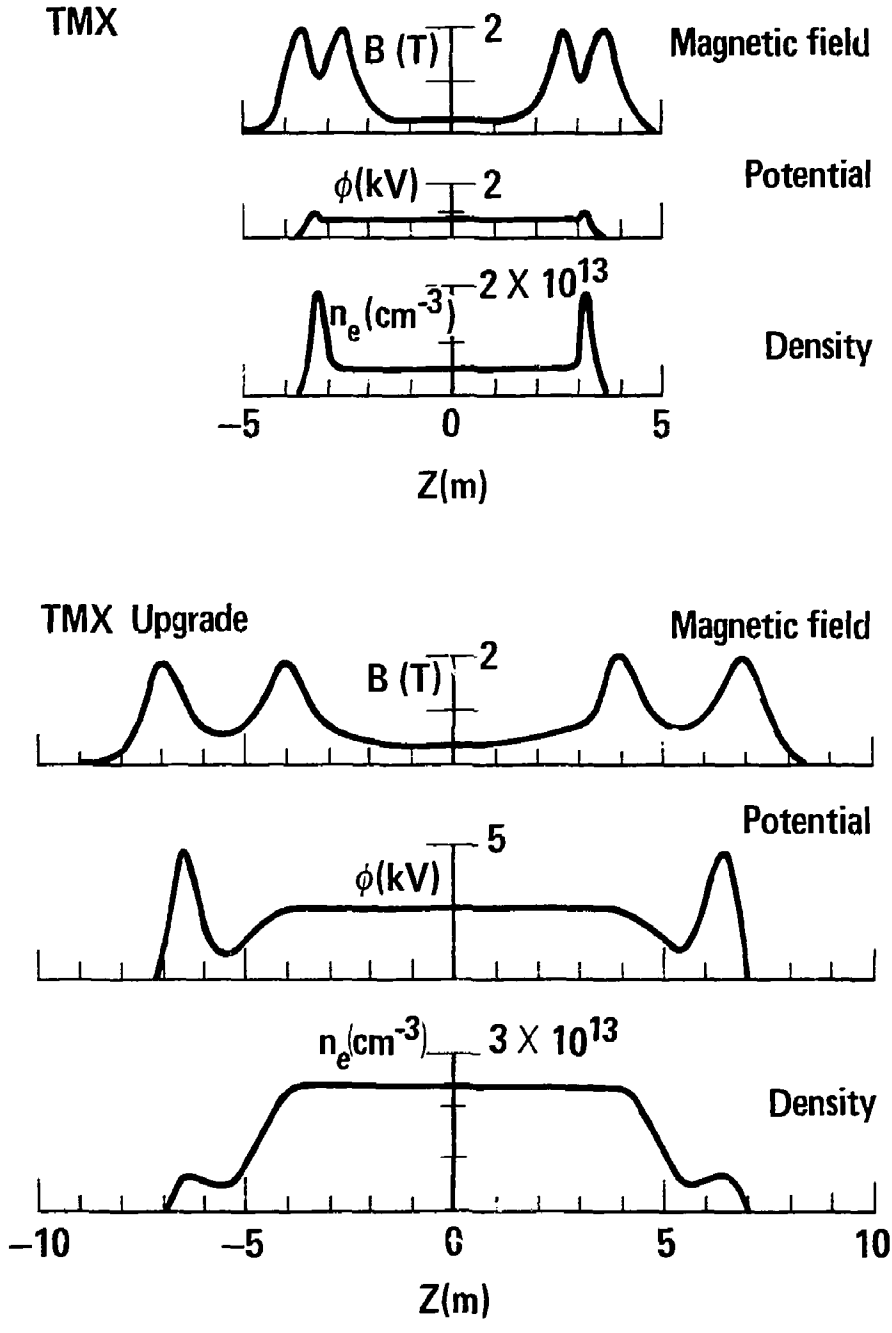

FIG. 1. Comparison of the axial magnetic field, potential, and density profiles generated in TMX to those projected for TMX Upgrade.

II. CHARACTERISTICS OF TMX UPGRADE

Machine parameters for TMX Upgrade are given in Table I. TMX has been modified and systems have been added or modifed as briefly described below. These improvements were needed to carry out the thermal-barrier experimental objectives outlined above. A schematic of TMX Upgrade is shown in Fig. 2.

The plug magnet system, shown in Fig. 3, was lengthened to allow access for neutral-beam injection at 45° in order to achieve microstability. To confine 45° injected ions, the plug mirror ratio was increased from 2:1 to 4:1. The magnetic field strength was selected to allow the use of commercially available 28-GHz gyrotrons for microwave heating. The central-cell field strength was increased to 0.3 T and has an axisymmetric rise in magnetic field to reduce resonant-neoclassical radial ion transport.

A high-power ECRH microwave heating system was added to generate magnetically confined electrons to form thermal barriers. The 28-GHz gyrotron system is also needed to raise the end-plug electron temperature to increase the confining electrostatic potential well.

Several changes were necessary in the neutral-beam system. Already mentioned was the capability for injection at 45° rather than 90° for microstability. Thermal-barrier pumping beams inject at 18°. Since the temperatures are higher and the plasma larger in TMX Upgrade, it was necessary to increase the output power of the neutral-beam system to 10 MW. To sustain plasmas for several confinement times, and to allow time for buildup, the beam duration was increased from 25 to 75 msec. TMX Upgrade will operate with hydrogen, rather than deuterium, in order to increase the central-cell radial confinement and to increase the heating rate of ions injected by central-cell neutral beams. The pump beams will, however, operate with deuterium for increased trapping efficiency.

TABLE 1. Comparison of major differences between TMX and TMX Upgrade.

	TMX	TMX Upgrade
Magnet System		
End plug midplane field	1.0 T	0.5 T
Plug mirror ratio	2:1	4:1
Plug length	0.9 m	3.0 m
Central-cell length	5.5 m	8.0 m
Central-cell field strength	0.2 T	0.3 T
Magnet power system	13 MW	26 MW
Overall machine length	15 m	22 m
Neutral-Beam System		
Duration	25 ms	75 ms
Maximum power	5 MW	10 MW
Plug injection angles	90^{o}	90^{o}, 65^{o}, 45^{o}, 18^{o}
Central-cell injection angles	90^{o}	90^{o}, 70^{o}, 58.5^{o}
ECRH System		
Number of gyrotrons	0	4
Maximum power per gyrotron	-	200 kW
Frequency	-	28 GHz
Vacuum System		
Volume	120	225 m^3
Pumping speed	3×10^7 l/s	5×10^7 l/s
Gas feed system	Pulsed	Programmable

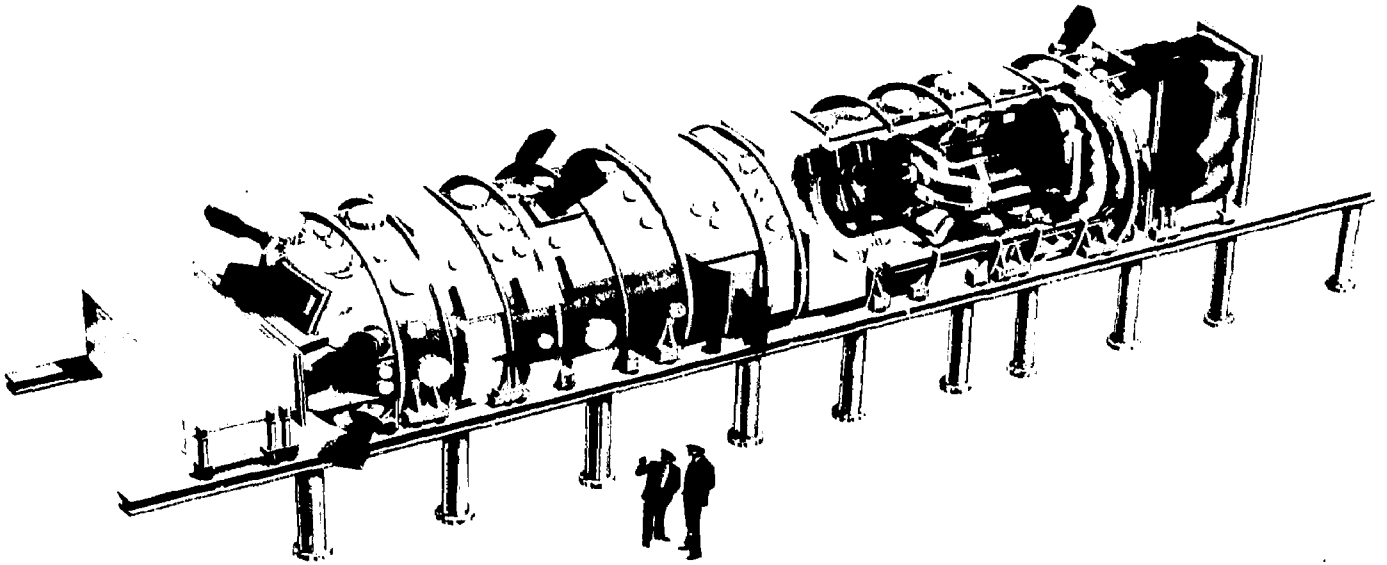

FIG. 2. Cutaway schematic of TMX Upgrade.

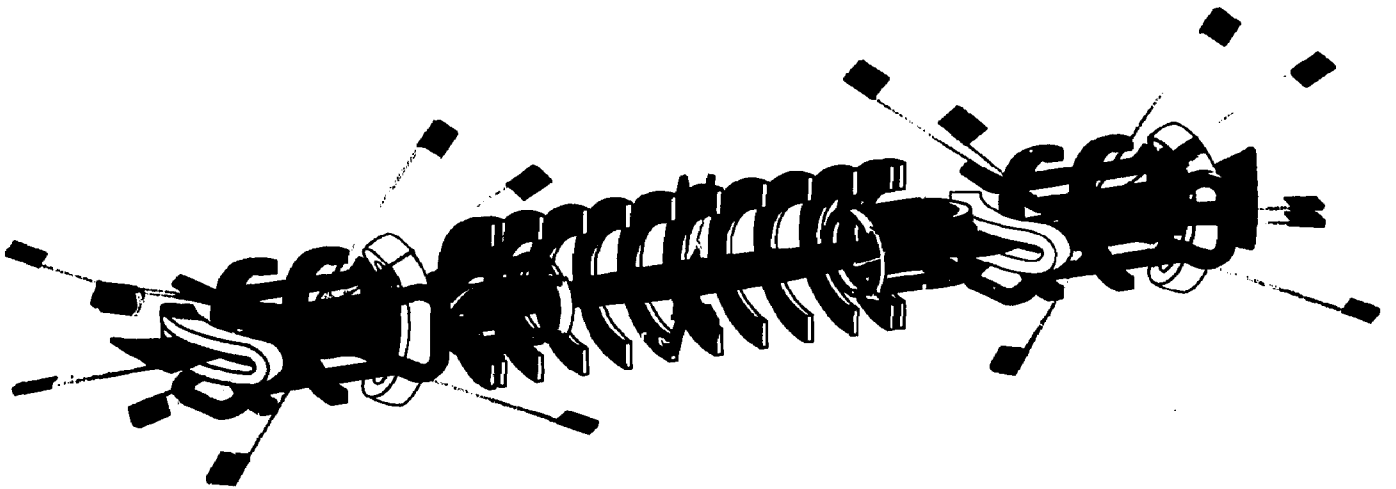

FIG. 3. The TMX Upgrade magnet and neutral-beam systems.

III. FORMATION OF A THERMAL BARRIER BY GENERATION OF AN AMBIPOLAR POTENTIAL PROFILE

The thermal-barrier concept improves the performance of tandem mirror systems by allowing larger electrostatic confining potentials to be established while at the same time allowing low-energy ions to penetrate into the end cells to improve their microstability. The thermal-barrier potential profile in the end cell of the TMX upgrade is shown in Fig. 4. Ions are injected at position (b) at approximately 45°. Consequently, the injected ions slosh back and forth creating density peaks at their turning points. Applying ECRH to the outer density peak in conjunction with a thermal barrier produces the final potential peak desired.

To maintain the sloshing-ion density profile, energetic ions that become deeply trapped must be pumped away, along with trapped ions accumulated by collisions among ions passing back and forth from the central cell. These trapped ions are pumped away by undergoing charge-exchange interactions with neutral beams located at each end of the machine. These neutral beams are aimed at 18° to the axis so that they are not mirror confined and pass through the end plugs. A charge-exchange collision between a trapped ion and an axially aimed neutral beam swaps a trapped ion for one that is not trapped. Charge-exchange collisions with the sloshing beams also provide pumping.

Details of the various populations of passing and trapped ions and electrons are shown in Fig. 5, including the magnetically trapped hot electrons (μ-trapped) that are created by applying ECRH at point (b) to depress the potential further and thereby block the flow of passing thermal electrons. This is essential to create a large potential difference ϕ_c between point (a) and the central cell,

Basic tandem potential profile

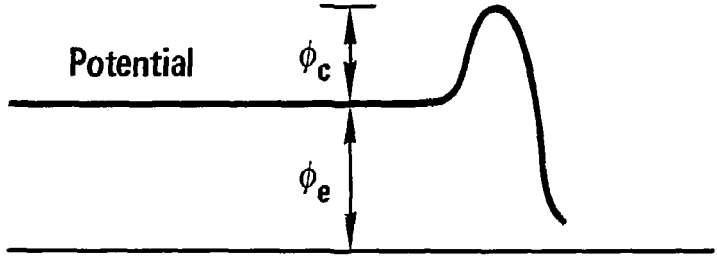

$$\Phi_c = T_{ep} \ln\left(\frac{n_p}{n_c}\right)$$

Thermal barrier potential profile

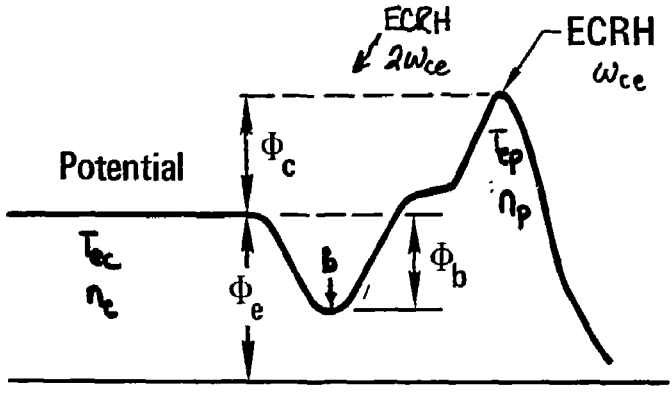

$$\Phi_c = T_{ep} \ln\left[\frac{n_p}{n_b^*}\left(\frac{T_{ec}}{T_{ep}}\right)^{1/2}\right] - T_{ec} \ln\left(\frac{n_c}{n_b^*}\right)$$

FIG. 4. Comparison of electrostatic potential barrier in a basic tandem mirror to that with a thermal barrier.

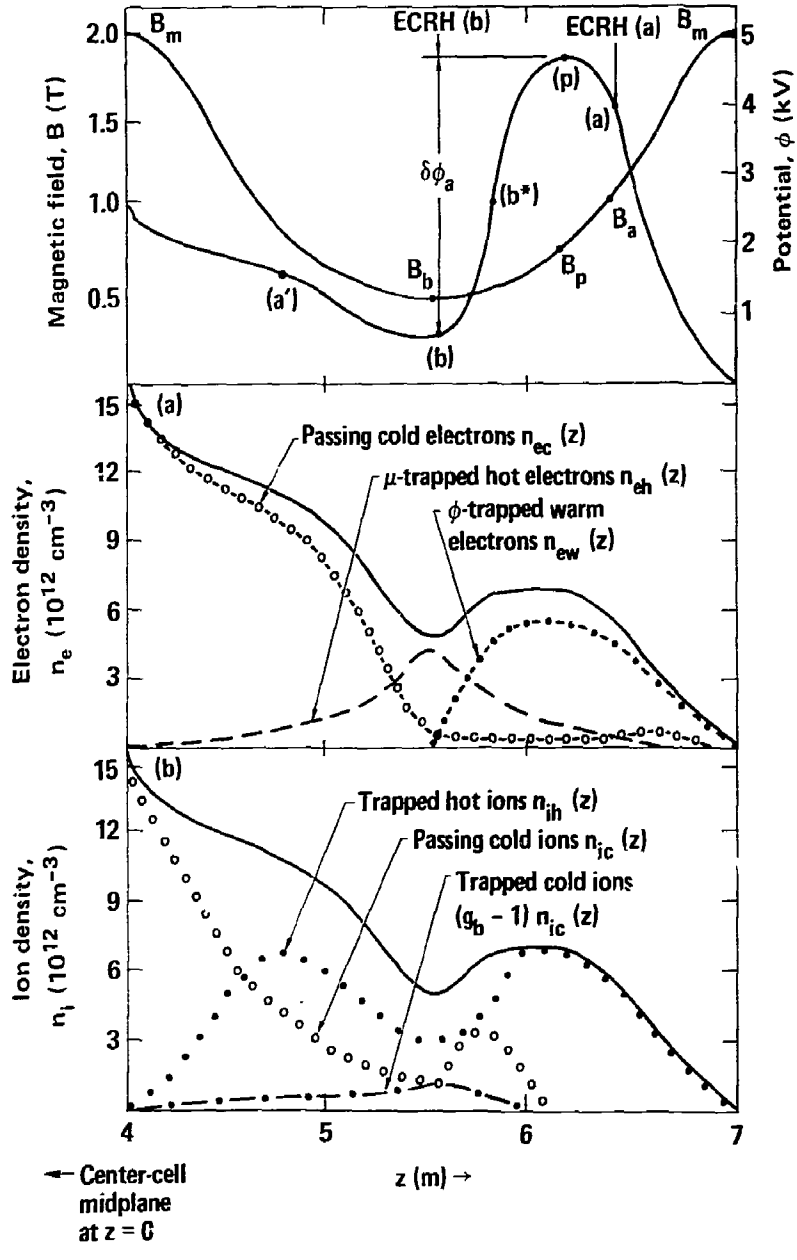

FIG. 5. Spatial distribution of ions and electrons in TMX Upgrade end cells.

$$\phi_c = T_{ep} \ln \left[\frac{n_p}{n_b^*} \left(\frac{T_{ec}}{T_{ep}} \right)^{1/2} \chi \right] - T_{ec} \ln \left(\frac{n_c}{n_b^*} \right) \quad . \tag{1}$$

Here n_b^* is the passing electron density at the position (b) and the subscripts e, c, and p refer to electron, central cell, and peak, respectively. The factor χ, described in Section IV, describes the effect of electron sources in the plug region. Under ideal circumstances, $\chi = 1$. To obtain the desired benefit from the thermal barrier requires $T_{ep} > T_{ec}$. Also as long as $n_b^* << n_b$ (good blockage of the thermal electrons), we can obtain a large value of ϕ_c even if the plug density n_p is less than the central-cell density n_c; namely, if $n_c > n_p > n_b >> n_b^*$.

Finally, from Fig. 5, we can see how the thermal-barrier designs discussed here lead to microstable configurations. As can be seen from the figure, the passing-ion and cold-trapped-ion populations extend deep into the end plug. Only the outer peak at the turning point of the hot ions is unprotected. The loss cone need not be filled everywhere, especially if locally $dB/dz \neq 0$.

IV. THE EFFECT OF NEUTRAL GAS ON PLASMA POTENTIAL

In this section we evaluate the effect of neutral gas on plasma potential and conclude that the vacuum-system requirements are similar to those imposed by other constraints, such as hot-ion charge exchange. Electron sources in the end plug, such as those generated by cold gas, degrade the confining electrostatic potential. The reason for this degradation is that electrons generated in the plug region are trapped in the electrostatic well and tend to balance the net positive charge of the electrostatic plug. The

factor X in the logarithm of Eq. (1) describes the effect of a source of electrons in the plug region:

$$X = \frac{1 + J_{AB}}{1 + C_{RF} \frac{n_p}{n_b} \left(\frac{T_{ec}}{T_{ep}}\right)^{1/2} J_{AB}} \quad , \tag{2}$$

where

$$J_{AB} = \frac{\sqrt{\pi}}{4} (1 + R) \frac{\tau_{ee} J_e}{C_{RF} n_{ep}} \quad ,$$

and

$$C_{RF} = 1 + D_{\perp RF}/D_{classical} \quad .$$

Here τ_{ee} is the large angle scattering time ($\tau_{ee} = 4 \times 10^8 \, T_{ew}^{3/2}/n_{ew}$), the mirror ratio ($R = B_b/B_a = 0.5$ for TMX Upgrade), and J_e is the electron production rate in the plug (cm^{-3}/s). The ratio of this rate to the rate at which electrons scatter out of the plug is J_{AB}. For no electron production ($J_e = 0$), $X = 1$. As J_e increases, X decreases, ($0 < X < 1$). The confining potential, ϕ_c, is plotted in Fig. 6 as a function of J_e for a typical set of TMX Upgrade parameters.

Figure 6 indicates that tolerable levels of cold electron production (J_e) in the plug are on the order of 10^{15} cm^{-3}/s. This rate results in roughly a 10% decrease of the confining potential. At larger values of J_e, the reduction is larger. By examining the plug-barrier region in TMX Upgrade, we can estimate the magnitude of J_e to be expected. The plasma volume in the end cell is approximately 100 liters, so a tolerable cold electron production rate in each end cell is about 16 amps.

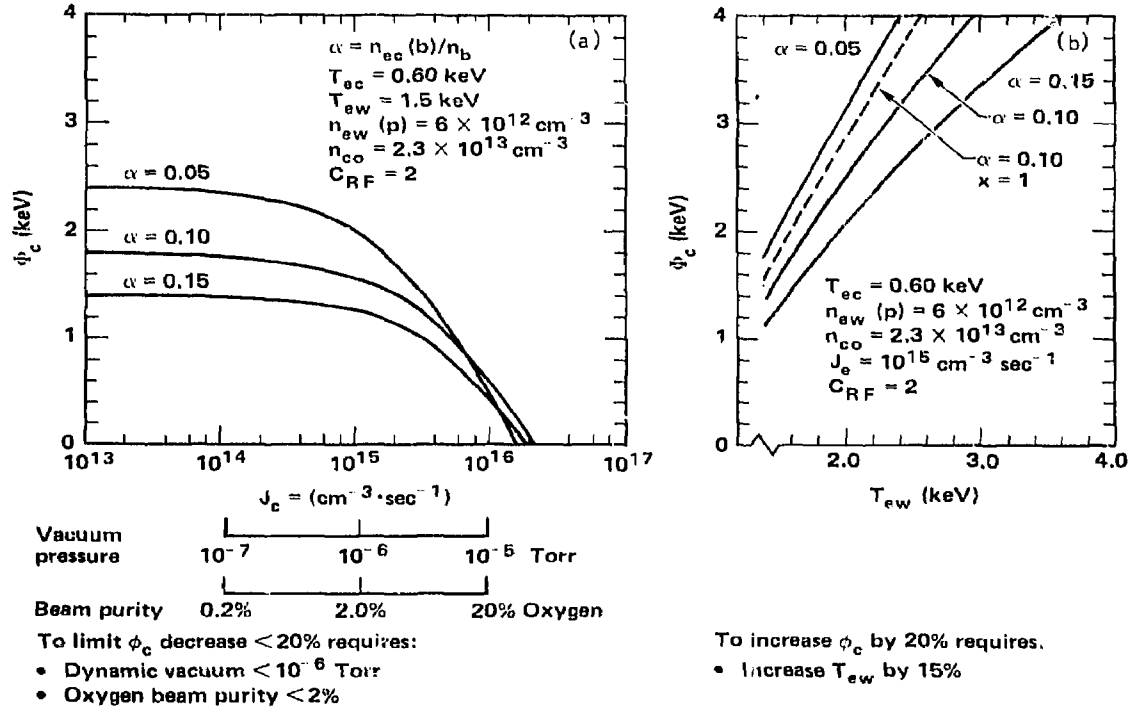

FIG. 6. This figure shows the sensitivity of the confining potential to (a) vacuum conditions and (b) electron temperature.

The sources of cold electrons in the plug are impurities and cold hydrogen gas, both of which can penetrate to the core of the plasma and be ionized there. On the basis of the 2XIIB and TMX experiments, the primary impurity in the plasma will most likely be oxygen injected by the neutral beams. The oxygen current fraction in the neutral-beam sources is presently about 2%. For 150 A of neutral-beam current, we can expect 3 A of oxygen to be injected into the end-cell plasma. Assuming each oxygen atom contributes 5 electrons to the end-cell plasma, the oxygen in the neutral beams would contribute 15 A of cold electrons to the end cell.

There are two sources for the cold hydrogen: the first is streaming gas from the neutral beams, and the second is reflux from the wall due to the energetic neutrals striking it. The nine neutral-beam sources in each end cell give a total of 6 A of streaming hydrogen to the plasma. The wall reflux comes from the charge-exchange products striking the walls and from the small fraction of the neutral beams that strike nearby walls. The charge-exchange current from the plasma is approximately 40 A. Of this, 8 A is incident on the plasma, assuming that 20% is not absorbed on the titanium-gettered walls. Thus, from the various sources of hydrogen gas, we can expect about 14 A of neutral atoms to impinge on the end-cell plasma. If all of these neutrals penetrate to the core of the plasma and are ionized, the electrons that would be produced (from this and from the impurities) would reduce the confining potential.

Most of the neutral-gas molecules penetrate to the center of the plasma where they also can be a source of electrons. That is, a neutral molecule has only a small probability of being ionized and magnetically trapped outside the plasma core since the plug density is only 7×10^{12} and the fan field thickness is only 8 cm. Setting the ionization rate of these molecules equal

to the maximum allowable electron-production rate, we calculate that the maximum hydrogen pressure permitted outside the plasma is 1×10^{-6} Torr.

In summary, cold gas and impurities, which penetrate to the center of the plasma in the plug region and are ionized there, can reduce the confining potential. The cold-electron production rate due to this ionization should be kept below 10^{15} cm^{-3}/s. The neutral pressure outside the plasma region must be less than 1×10^{-6} Torr. Alternatively, the ionization current in the end cell must be less than 16 A. Oxygen injected with the beam could contribute this amount. These considerations have led us to improve the vacuum system in TMX Upgrade and to decrease the neutral-beam impurities. Since these effects are additive, TMX Upgrade design requirements are more stringent than outlined here. Our design includes better pumping of the cold gas from the neutral beams and titanium-gettered walls to minimize gas recycling. To compensate for the reduction in confining potential, the plug electron temperature can be increased with microwave heating as illustrated in Fig. 6.

V. ELECTRON-CYCLOTRON RESONANCE HEATING (ECRH)

TMX Upgrade will employ four 200-kW, 28-GHz gyrotrons. At each end, one gyrotron will create the magnetically confined barrier electrons and another will heat the electrons in the potential peak. As shown in Fig. 7, microwave horns will illuminate the 0.5-T barrier region for second-harmonic heating and the 1.0-T plug region for fundamental heating. Our design allows us to launch either ordinary or extraordinary waves in order to optimize the absorption profile.

Ray-tracing calculations are being carried out to determine optimum antenna locations, aiming, and polarization. These calculations include the

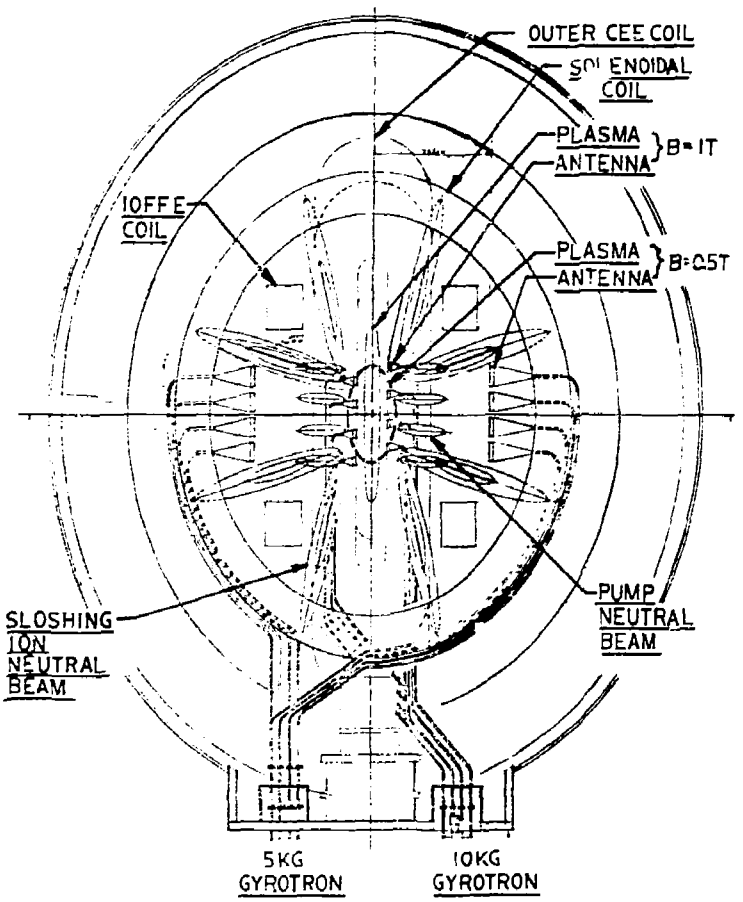

FIG. 7. This drawing shows how microwave power and neutral beams deliver power through the vacuum tanks and magnets to the plasma.

spatial variations in magnetic field strength and plasma electron density. Results of such calculations for the extraordinary wave are shown in Figs. 8 and 9.

Figure 8 shows the ray trajectories for second-harmonic heating at the 0.5-T resonance. The two curves show examples of the illumination of the resonant surface as the mirror ratio for resonance is varied (for reasons described later). The microwave aiming is adjusted to intersect the resonant surface. These calculations have shown that the ray trajectories of the microwave beam are a reasonable match to the absorption profile of the hot electrons at the desired temperature and density. (T_{eh} ~ 50 keV, n_{eh} ~ 4×10^{12}). They also show strong ray bending if the density appoaches cutoff ($n_{ec} = 5 \times 10^{12}$).

Figure 9 shows ray trajectories for fundamental heating at the 1.0-T potential plug. The two calculations show the effect of spatial shift of the resonant location with beta shift due to an increase in density from 1 to 7 $\times$ 10^{12} cm^{-3}. From such calculations we conclude that absorption of the extraordinary mode should be highly efficient. Because of the magnetic geometry for mirrors ($\underline{\nabla B} \parallel \underline{B}$) the rays tend to follow the resonance surface leading to enhanced absorption.

We used such ray-tracing calculations to design the microwave antenna system. We concluded that the extraordinary wave may be very strongly absorbed on the edge of the plasma, depending upon the radial electron-temperature profile, and that it may be necessary to use the ordinary wave in order to penetrate into the central region. The ordinary wave's absorption is about 30%. Our antenna system with 12 horns will allow us to vary the amount of power in each polarization in order to control the radial absorption profile.

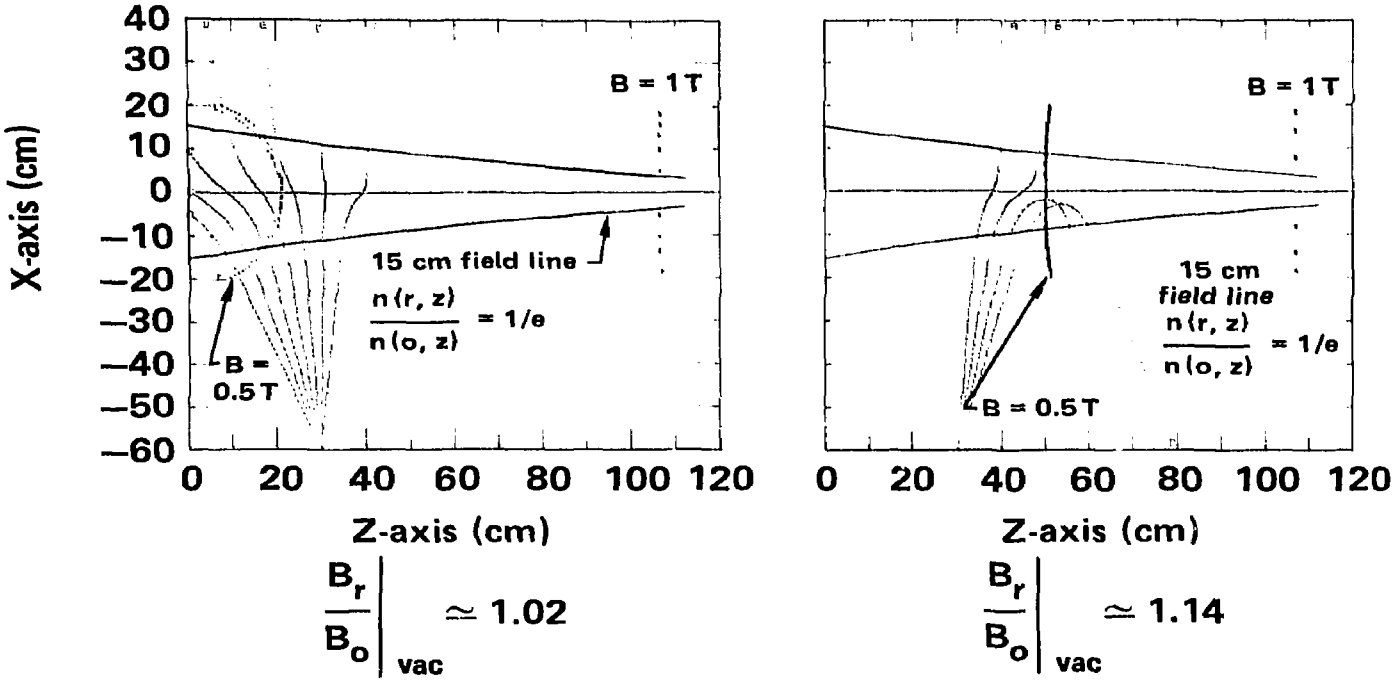

Ray trajectories for several resonant mirror ratios. Extraordinary mode, $\omega_{rf} = 2\omega_{ce}$. Midplane peak density $n_o = 4.1 \times 10^{12}$ cm^{-3}.

FIG. 8. Ray trajectories for second-harmonic extraordinary wave absorption at two different mirror ratios.

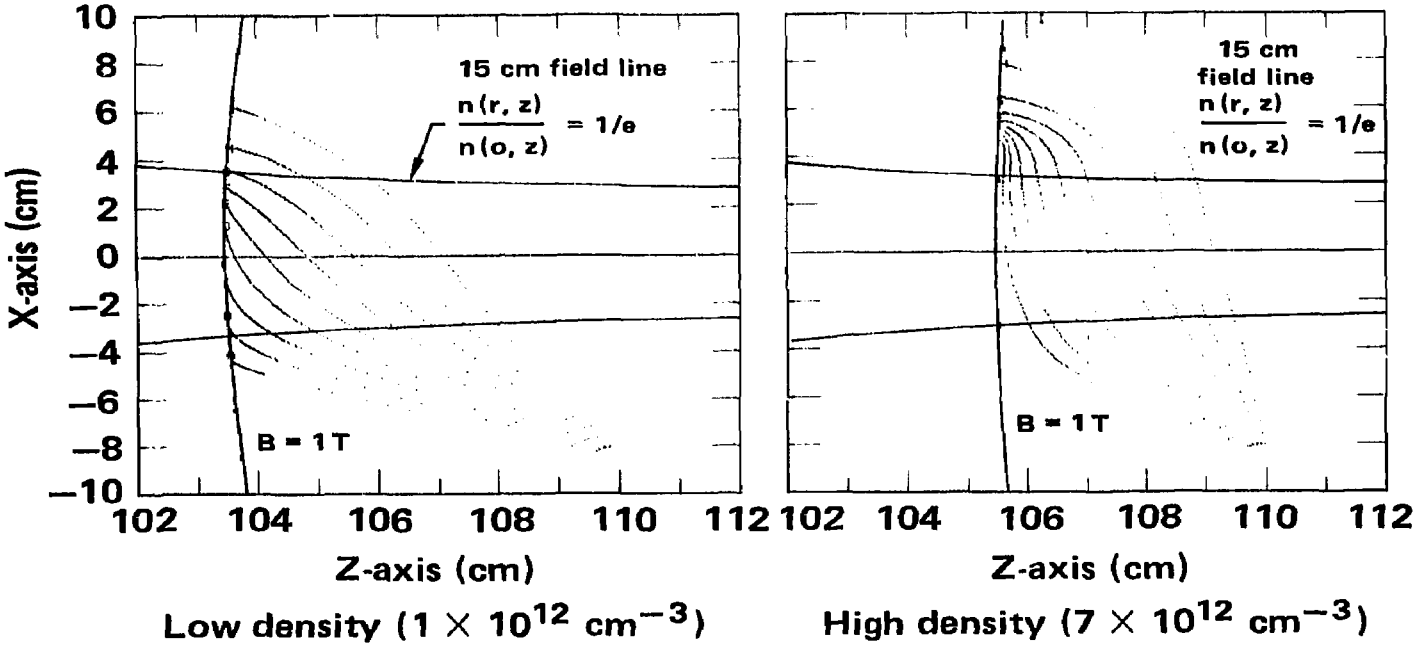

Ray trajectories for low and high density plasmas showing estimated beta-shift of resonant surface. Extraordinary mode, $\omega_{rf} = \omega_{ce}$

FIG. 9. Fundamental-frequency extraordinary wave ray trajectories for low and high density plasmas. This comparison shows the effect of beta-shift of the resonant surface.

The localization of the incident microwave power in the thermal barrier allows us to control both ECRH runaway and electron anisotropy as illustrated in Fig. 10.

If electron runaway is not inhibited, the electron beta would be due to a small number of energetic electrons. In this event, the thermal barrier would be inefficient, since a higher fraction of passing electrons would exist to transfer heat from the plug to the central cell. Localized electron heating inhibits runaway since energetic electrons will be detuned from cyclotron resonance.

Electron anisotropy must also be controlled to prevent excessive power loss due to a class of electron microinstabilities driven by anisotropy. Sufficient parallel temperature stabilizes the electron microinstabilities. Off-midplane heating will produce an effective parallel temperature, as well as a perpendicular temperature. Varying the midplane field B_o, relative to the resonance field B_r controls the anisotropy, $T_{\parallel}/T_{\perp} = B_r/B_o - 1$. Control of other modes, such as the upper-hybrid loss-cone mode, are under study.

To determine the heating rates, steady-state temperatures, and electron velocity-distribution functions for microstability analysis, Fokker Planck and Monte Carlo codes have been developed. The preliminary results from these codes by Matsuda and Kognlein are qualitatively similar and indicate that the required electron energies and densities can be achieved within TMX Upgrade time scales. Ongoing work with these codes is including Doppler-shift effects and more self-consistent electrostatic-potential effects.

In summary, ray-tracing and heating calculations have been and are being used to design the TMX Upgrade ECRH system and to guide experimental plans and ultimately, data analysis. These calculations have already led us away from several pitfalls and directed us toward several promising approaches that are

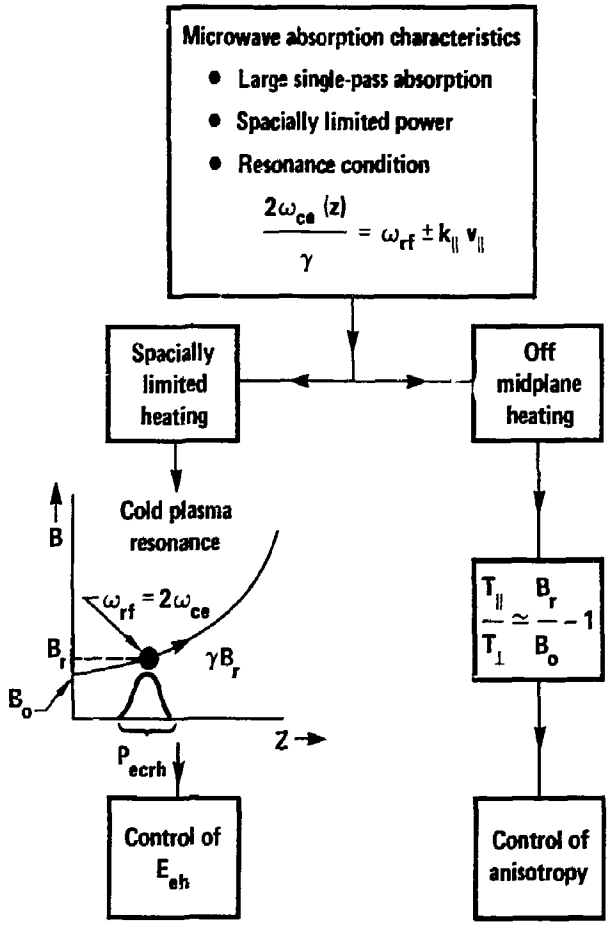

FIG. 10. Outline of the method used to control thermal-barrier hot-electron energy and anisotropy.

now being evaluated in greater detail. At final operating temperatures, absorption of the extraordinary wave is strong, so we are providing the capability of launching a controllable fraction of ordinary wave power.

VI. SUMMARY

We have described the formation and control of plasma potentials in the TMX Upgrade tandem mirror. A potential depression between the end plug and central cell forms a thermal barrier that allows the end-plug electron temperature to be increased to about twice that of the central cell. The higher plug electron temperature generates a higher plug electrostatic potential. The larger potential barrier should allow us to reach higher central-cell ion temperatures and confinement times than were possible in TMX.

We have evaluated the consequences of cold gas on potential formation and found the TMX Upgrade vacuum requirements to be comparable to those based on cold-gas charge exchange of hot ions.

Calculations of energy absorption and control in ECRH have indicated that the required energies and densities can be achieved and controlled. Our calculations show high absorption of the extraordinary wave at the plasma boundary so we are planning to employ a variable fraction of ordinary wave power to control the radial power-deposition profile. Electron energy control appears acnievable by localized electron heating.

At the time of the Mirror League meeting next spring, we expect to be able to report on initial experimental results from TMX Upgrade. By that time, we expect to have begun our first plasma experiments and to be beginning experiments to form and control ambipolar potentials in a thermal-barrier tandem mirror.

FOOTNOTES

*This work was performed under the auspices of the U.S. Department of Energy by Lawrence Livermore National Laboratory under Contract No. W-7405-ENG-48.

†Permanent address: Massachusetts Institute of Technology.

MEH:sc